Lepton polarization asymmetry in radiative dileptonic *B*-meson decays in the minimal supersymmetric standard model

S. Rai Choudhury,* Naveen Gaur,† and Namit Mahajan‡
Department of Physics and Astrophysics, University of Delhi, Delhi 110 007, India
(Received 12 April 2002; published 17 September 2002)

In this paper we study the polarization asymmetries of the final state lepton in the radiative dileptonic decay of the B meson ($B_s \to \ell^+ \ell^- \gamma$) in the framework of the minimal supersymmetric standard model (MSSM) and various other unified models within the framework of the MSSM, e.g., MSUGRA, SUGRA (where the condition of universality of scalar masses is relaxed), etc. Lepton polarization, in addition to having a longitudinal component (P_L), can have two other components P_T and P_N lying in and perpendicular to the decay plane, which are proportional to m_ℓ and hence are significant for the final state being $\mu^+ \mu^-$ or $\tau^+ \tau^-$. We analyze the dependence of these polarization asymmetries on the parameters of the various models.

DOI: 10.1103/PhysRevD.66.054003 PACS number(s): 13.20.He, 12.60.Jv, 13.88.+e

I. INTRODUCTION

Flavor changing neutral current (FCNC) induced *B*-meson rare decays provide a unique testing ground for the standard model (SM) improved by QCD corrections via operator product expansion (for a review and complete set of references see [1]). Studies of rare B decays can give precise information about various fundamental parameters of the SM such as Cabibbo-Kobayashi-Maskawa (CKM) matrix elements, leptonic decay constants, etc. In addition to this, rare B decays can also give information about various extensions of the SM such as the two Higgs doublet model (2HDM) [2–5], minimal supersymmetric standard model (MSSM) [6–13], etc. After the first observation of the penguin induced decay $B \to X_s \gamma$ and the corresponding exclusive decay channel $B \to K^* \gamma$ by CLEO [14], rare decays have begun to play an important role in particle physics phenomenology.

Among the rare B decays, $B_s \to \ell^+ \ell^- \gamma$ ($\ell = e, \mu, \tau$) are of special interest due to their relative cleanliness and sensitivity to new physics. They have been extensively studied within the SM [16–18] and beyond [2]. In the mode $B_s \to \ell^+ \ell^- \gamma$, one can study many experimentally accessible quantities associated with final state leptons and a photon, e.g., lepton pair invariant mass spectrum, lepton pair forward backward asymmetry, photon energy distribution, and various polarization asymmetries (like longitudinal, transverse, and normal). The final state leptons in the radiative decay mode $B_s \to \ell^+ \ell^- \gamma$, apart from having longitudinal polarization, can have two more components of polarization (P_T is the component of the polarization lying in the decay plane and P_N is the one that is normal to the decay plane) [19]. Both P_N and P_T remain nontrivial for the $\mu^+ \mu^-$ and $\tau^+ \tau^-$ channel since they are proportional to the lepton mass, m_ℓ. The different components of the polarization, i.e., P_L, P_N, P_T involve different combinations of Wilson coefficients and hence contain independent information. For this reason confronting the polarization results with experiments are important investigations of the structure of SM and for establishing new physics beyond it. The radiative process $B_s \to \ell^+ \ell^- \gamma$ has been extensively studied in 2HDM and SUSY by various people [2,7] and the importance of the neutral Higgs bosons (NHBs) has been emphasized in the decay mode with μ and τ pairs in the final state. In this work we study various polarization asymmetries associated with final state lepton (considering lepton to be either muon or tau) with special focus on the NHB effects.

$B_s \to \ell^+ \ell^- \gamma$ decay is induced by the pure leptonic decay $B_s \to \ell^+ \ell^-$ which suffers from helicity suppression for light leptons ($\ell = e, \mu$). But in the radiative mode ($B_s \to \ell^+ \ell^- \gamma$) this helicity suppression is overcome because the lepton pair by itself does not carry the available four momentum. For this reason, one can expect $B_s \to \ell^+ \ell^- \gamma$ to have a relatively large branching ratio compared to the nonradiative mode despite an extra factor of α. In MSSM, the situation for pure dileptonic modes ($B_s \to \ell^+ \ell^-$) becomes different, specially if $\ell = \mu,\ \tau$ and $\tan\beta$ is large [4,6,7]. This is because in MSSM the scalar and pseudoscalar Higgs coupling to the leptons is proportional to $m_\ell \tan\beta$ and thus can be large for $\ell = \mu,\ \tau$ and for large $\tan\beta$. The effect of NHBs has been studied in great detail in various leptonic decay modes [2–9,11,15]. The effect of NHBs on radiative mode $B_s \to \ell^+ \ell^- \gamma$ has also been studied in 2HDM [2] and SUSY [7]. Here we will focus on the NHB effects on various polarization asymmetries within the framework of the MSSM.

This paper is organized as follows. In Sec. II we first present the leading order (LO) QCD corrected effective Hamiltonian for the quark level process $b \to s \ell^+ \ell^- \gamma$ including NHB effects leading to the corresponding matrix element and dileptonic invariant mass distribution. In Sec. III, the three polarization asymmetries associated with the final state lepton are calculated. Section IV contains a discussion of the numerical analysis of the polarization asymmetries and their dependence on various parameters of the theory, focusing again mainly on NHB effects in the large $\tan\beta$ regime.

II. DILEPTON INVARIANT MASS DISTRIBUTION

The exclusive decay $B_s \to \ell^+ \ell^- \gamma$ can be obtained from the inclusive decay $b \to s \ell^+ \ell^- \gamma$ and further from b

*Electronic address: src@ducos.ernet.in
†Electronic address: naveen@physics.du.ac.in
‡Electronic address: nmahajan@physics.du.ac.in

$\to s\ell^+\ell^-$. To do this a photon has to be attached to any charged internal or external line in the Feynman diagrams for $b\to s\ell^+\ell^-$. As pointed out by Eilam *et al.* [16], contributions coming from the attachment of a photon to any charged internal line will be suppressed by a factor of m_b^2/M_W^2 in the Wilson coefficient and hence can be safely neglected. So we only consider the cases when the photon is hooked to initial quark lines and final lepton lines. To start off, the effective Hamiltonian relevant for $b\to s\ell^+\ell^-$ is [2–4,6–9]:

$$\begin{aligned}\mathcal{H}_{\rm eff}=&\frac{\alpha G_F}{2\sqrt{2}\pi}V_{tb}V_{ts}^*\Big\{-2C_7^{\rm eff}\frac{m_b}{p^2}\bar{s}i\sigma_{\mu\nu}p^\nu(1+\gamma_5)b\bar{\ell}\gamma^\mu l\\&+C_9^{\rm eff}\bar{s}\gamma_\mu(1-\gamma_5)b\bar{\ell}\gamma^\mu\ell\\&+C_{10}\bar{s}\gamma_\mu(1-\gamma_5)b\bar{\ell}\gamma^\mu\gamma_5\ell\\&+C_{Q_1}\bar{s}(1+\gamma_5)b\bar{\ell}\ell+C_{Q_2}\bar{s}(1+\gamma_5)b\bar{\ell}\gamma_5\ell\Big\},\end{aligned}\tag{2.1}$$

where $p=p_1+p_2$ is the sum of momenta of ℓ^- and ℓ^+ and V_{tb}, V_{ts} are CKM factors. The Wilson coefficients $C_7^{\rm eff}$, $C_9^{\rm eff}$, and C_{10} are given in [12,20]. Wilson coefficients C_{Q_1} and C_{Q_2} are given in [6–8,11]. In addition to the short distance corrections included in the Wilson coefficients, there are some long distance effects also, associated with real $c\bar{c}$ resonances in the intermediate states. This is taken into account by using the prescription given in [21], namely by using the Breit-Wigner form of resonances that add on to $C_9^{\rm eff}$:

$$C_9^{(res)}=\frac{-3\pi}{\alpha^2}\kappa_V\sum_{V=J/\psi,\psi',\ldots,}\frac{M_V Br(V\to\ell^+\ell^-)\Gamma^V_{\rm total}}{(s-M_V^2)+i\Gamma^V_{\rm total}M_V},\tag{2.2}$$

there are six known resonances in the $c\bar{c}$ system that can contribute.[1] The phenomenological factor κ_V is taken as 2.3 in numerical calculations [19,21].

Using Eq. (2.1) we calculate the matrix elements for the decay mode $B_s\to\ell^+\ell^-\gamma$. When the photon is hooked to the initial quark lines, the corresponding matrix element can be written as

$$\begin{aligned}\mathcal{M}_1=&\frac{\alpha^{3/2}G_F}{\sqrt{2\pi}}V_{tb}V_{ts}^*\{[A\varepsilon_{\mu\alpha}\beta_\sigma\epsilon^{*\alpha}p^\beta q^\sigma+iB(\epsilon_\mu^*(pq)\\&-(\epsilon^*p)q_\mu)]\bar{\ell}\gamma^\mu\ell\\&+[C\varepsilon_{\mu\alpha\beta\sigma}\epsilon^{*\alpha}p^\beta q^\sigma+iD(\epsilon_\mu^*(pq)\\&-(\epsilon^*p)q_\mu)]\bar{\ell}\gamma^\mu\gamma_5\ell\},\end{aligned}\tag{2.3}$$

where A, B, C, and D are related to the form factor definition and are defined in Appendix Eqs. (B1)–(B4). Here ϵ_μ and q_μ are the polarization vector and four momentum of the photon, respectively, and p is the momentum transfer to the lepton pair, i.e., the sum of momenta of ℓ^+ and ℓ^-. We can very easily see from the structure of Eq. (2.3) that neutral scalars do not contribute to $\mathcal{M}_1$. This is due to Eq. (B4) given in Appendix B.

When the photon is radiated from either of the lepton lines we get the contribution due to C_{10} along with scalar and pseudoscalar interactions, i.e., C_{Q_1} and C_{Q_2}. Using Eqs. (B6)–(B8) of Appendix B [2,7] the corresponding matrix element is

$$\begin{aligned}\mathcal{M}_2=&\frac{\alpha^{3/2}G_F}{\sqrt{2\pi}}V_{tb}V_{ts}^*i2m_\ell f_{B_s}\Big\{\Big(C_{10}+\frac{m_{B_s}^2}{2m_\ell m_b}C_{Q_2}\Big)\bar{\ell}\Big[\frac{\not\epsilon\not P_{B_s}}{2p_2q}-\frac{\not P_{B_s}\not\epsilon}{2p_1q}\Big]\gamma_5\ell\\&+\frac{m_{B_s}^2}{2m_\ell m_b}C_{Q_1}\Big[2m_\ell\Big(\frac{1}{2p_1q}+\frac{1}{2p_2q}\Big)\bar{\ell}\not\epsilon\ell+\bar{\ell}\Big(\frac{\not\epsilon\not P_{B_s}}{2p_2q}-\frac{\not P_{B_s}\not\epsilon}{2p_1q}\Big)\ell\Big]\Big\},\end{aligned}\tag{2.4}$$

where P_{B_s} and f_{B_s} are the four momentum and decay constant of the B_s meson and p_1 and p_2 are the four momenta of ℓ^- and ℓ^+, respectively.

The final matrix element of $B_s\to\ell^+\ell^-\gamma$ decay thus is

$$\mathcal{M}=\mathcal{M}_1+\mathcal{M}_2.\tag{2.5}$$

From this matrix element we can get the square of the matrix element as

[1]All these six resonances will contribute to the channel $B_s\to\mu^+\mu^-\gamma$ whereas in the mode $B_s\to\tau^+\tau^-\gamma$ all but the lowest one $J/\Psi(3097)$ will contribute because the mass of this resonance is less than the invariant mass of the lepton pair $(4m_\ell^2)$.

$$|\mathcal{M}|^2=|\mathcal{M}_1|^2+|\mathcal{M}_2|^2+2\,\mathrm{Re}(\mathcal{M}_1\mathcal{M}_2^*) \tag{2.6}$$

with

$$|\mathcal{M}_1|^2=4\left|\frac{\alpha^{3/2}G_F}{\sqrt{2\pi}}V_{tb}V_{ts}^*\right|^2\{[|A|^2+|B|^2][p^2((p_1q)^2+(p_2q)^2)+2m_\ell^2(pq)^2]+[|C|^2+|D|^2][p^2((p_1q)^2+(p_2q)^2)$$

$$-2m_\ell^2(pq)^2]+2\,\mathrm{Re}(B^*C+A^*D)p^2((p_2q)^2-(p_1q)^2)\}, \tag{2.7}$$

$$\begin{aligned}|\mathcal{M}_2|^2=4\left|\frac{\alpha^{3/2}G_F}{\sqrt{2\pi}}V_{tb}V_{ts}^*\right|^2 f_{B_s}^2m_\ell^2\Bigg[&\left(C_{10}+\frac{m_{B_s}^2}{2m_\ell m_b}C_{Q_2}\right)\Bigg\{8+\frac{1}{(p_1q)^2}(-2m_{B_s}^2m_\ell^2-m_{B_s}^2p^2+p^4+2p^2(p_2q))\\&+\frac{1}{(p_1q)}(6p^2+4(p_2q))+\frac{1}{(p_2q)^2}(-2m_{B_s}^2m_\ell^2-m_{B_s}^2p^2+p^4+2p^2(p_1q))+\frac{1}{(p_2q)}(6p^2+4(p_1q))\\&+\frac{1}{(p_1q)(p_2q)}(-4m_{B_s}^2m_\ell^2+2p^4)\Bigg\}\\&+\left(\frac{m_{B_s}^2}{2m_\ell m_b}C_{Q_1}\right)\Bigg\{8+\frac{1}{(p_1q)^2}(6m_{B_s}^2m_\ell^2+8m_\ell^4-m_{B_s}^2p^2-8m_\ell^2p^2+p^4-8m_\ell^2(p_2q)+2p^2(p_2q))\\&+\frac{1}{(p_1q)}(-40m_\ell^2+6p^2+4(p_2q))+\frac{1}{(p_2q)^2}(6m_{B_s}^2m_\ell^2+8m_\ell^4-m_{B_s}^2p^2-8m_\ell^2p^2+p^4-8m_\ell^2(p_1q)\\&+2p^2(p_1q))+\frac{1}{(p_2q)}(-40m_\ell^2+6p^2+4(p_1q))+\frac{1}{(p_1q)(p_2q)}(4m_{B_s}^2m_\ell^2+16m_\ell^4-16m_\ell^2p^2+2p^4)\Bigg\}\Bigg],\end{aligned} \tag{2.8}$$

$$\begin{aligned}2\,\mathrm{Re}(\mathcal{M}_1\mathcal{M}_2^*)=16\left|\frac{\alpha^{3/2}G_F}{\sqrt{2\pi}}V_{tb}V_{ts}^*\right|^2 f_{B_s}m_\ell^2\Bigg[&\left(C_{10}+\frac{m_{B_s}^2}{2m_\ell m_b}C_{Q_2}\right)\Bigg\{-\mathrm{Re}(A)\,\frac{(p_1q+p_2q)^3}{(p_1q)(p_2q)}\\&+\mathrm{Re}(D)\,\frac{(pq)^2(p_1q-p_2q)}{(p_1q)(p_2q)}\Bigg\}+\left(\frac{m_{B_s}^2}{2m_\ell m_b}C_{Q_1}\right)\Bigg\{\mathrm{Re}(B)\,\frac{1}{(p_1q)(p_2q)}(-(pq)^3-2(p_1p_2)(p_1q)^2\\&-2(p_1p_2)(p_2q)^2+4m_\ell^2(p_1q)(p_2q))+\mathrm{Re}(C)\,\frac{(pq)^2(p_1q-p_2q)}{(p_1q)(p_2q)}\Bigg\}\Bigg].\end{aligned} \tag{2.9}$$

The differential decay rate of $B_s\to\ell^+\ell^-\gamma$ as a function of invariant mass of dileptons is given by

$$\frac{d\Gamma}{d\hat{s}}=\left|\frac{\alpha^{3/2}G_F}{2\sqrt{2\pi}}V_{tb}V_{ts}^*\right|^2\frac{m_{B_s}^5}{16(2\pi)^3}(1-\hat{s})\sqrt{1-\frac{4\hat{m}_\ell^2}{\hat{s}}}\,\Delta, \tag{2.10}$$

with Δ defined as

$$\Delta=\frac{4}{3}m_{B_s}^2(1-\hat{s})^2[(|A|^2+|B|^2)(2\hat{m}_\ell^2+\hat{s})+(|C|^2+|D|^2)(-4\hat{m}_\ell^2+\hat{s})]$$
$$+\frac{64f_{B_s}^2\hat{m}_\ell^2}{m_{B_s}^2}\left(C_{10}+\frac{m_{B_s}^2}{2m_\ell m_b}C_{Q_2}\right)^2\frac{\left[(1-4\hat{m}_\ell^2+\hat{s}^2)\ln(\hat{z})-2\hat{s}\sqrt{1-\frac{4\hat{m}_\ell^2}{\hat{s}}}\right]}{(1-\hat{s})^2\sqrt{1-\frac{4\hat{m}_\ell^2}{\hat{s}}}}$$
$$-\frac{64f_{B_s}^2\hat{m}_\ell^2}{m_{B_s}^2}\left(\frac{m_{B_s}^2}{2m_\ell m_b}C_{Q_1}\right)^2\frac{\left[(-1+12\hat{m}_\ell^2-16\hat{m}_\ell^4-\hat{s}^2)\ln(\hat{z})+(-2\hat{s}-8\hat{m}_\ell^2\hat{s}+4\hat{s}^2)\sqrt{1-\frac{4\hat{m}_\ell^2}{\hat{s}}}\right]}{(1-\hat{s})^2\sqrt{1-\frac{4\hat{m}_\ell^2}{\hat{s}}}}$$
$$+32f_{B_s}\hat{m}_\ell^2\left(C_{10}+\frac{m_{B_s}^2}{2m_\ell m_b}C_{Q_2}\right)\mathrm{Re}(A)\frac{\ln(\hat{z})}{\sqrt{1-\frac{4\hat{m}_\ell^2}{\hat{s}}}}$$
$$-32f_{B_s}\hat{m}_\ell^2\left(\frac{m_{B_s}^2}{2m_\ell m_b}C_{Q_1}\right)\mathrm{Re}(B)\frac{\left[(1-4\hat{m}_\ell^2+\hat{s})\ln(\hat{z})-2\hat{s}\sqrt{1-\frac{4\hat{m}_\ell^2}{\hat{s}}}\right]}{\sqrt{1-\frac{4\hat{m}_\ell^2}{\hat{s}}}},\tag{2.11}$$

where $\hat{s}=p^2/m_{B_s}^2$, $\hat{m}_\ell^2=m_\ell^2/m_{B_s}^2$, and $\hat{z}=[1+\sqrt{1-(4\hat{m}_\ell^2/\hat{s})}]/[1-\sqrt{1-(4\hat{m}_\ell^2/\hat{s})}]$ are dimensionless quantities.

III. LEPTON POLARIZATION ASYMMETRIES

We now compute the lepton polarization asymmetries from the four Fermi interaction defined in the matrix element Eqs. (2.3) and (2.4). For this we need to calculate the polarized rates corresponding to different lepton polarizations. These rates are obtained by introducing spin projection operators defined by $N=1/2(1+\gamma_5 \not{S}_x)$, where index $x=L$, N, T and corresponds to longitudinal, normal, and transverse polarization states, respectively. The orthogonal unit vectors, S_x, defined in the rest frame of ℓ^- read [19]

$$S_L^\mu\equiv(0,\mathbf{e}_L)=\left(0,\frac{\mathbf{p}_1}{|\mathbf{p}_1|}\right),$$
$$S_N^\mu\equiv(0,\mathbf{e}_N)=\left(0,\frac{\mathbf{q}\times\mathbf{p}_1}{|\mathbf{q}\times\mathbf{p}_1|}\right),\tag{3.1}$$
$$S_T^\mu\equiv(0,\mathbf{e}_T)=(0,\mathbf{e}_N\times\mathbf{e}_L),$$

where $\mathbf{p}_1$ and $\mathbf{q}$ are the three momenta of ℓ^- and the photon in the center-of-mass (c.m.) frame of the $\ell^-\ell^+$ system. Furthermore, it is quite obvious to note that $S_x\cdot p_1=0$. Now boosting all three vectors given in Eq. (3.1) to the dilepton rest frame, only the longitudinal vector will get boosted while the other two (normal and transverse) will remain the same. The longitudinal vector after boost becomes[2]

$$S_L^\mu=\left(\frac{|\mathbf{p}_1|}{m_\ell},\frac{E_1\mathbf{p}_1}{m_\ell|\mathbf{p}_1|}\right).\tag{3.2}$$

We can now calculate the polarization asymmetries by using the spin projectors for ℓ^- as $1/2(1+\gamma_5\not{S})$. The lepton polarization asymmetries are defined as

$$P_x(\hat{s})\equiv\frac{\frac{d\Gamma(S_x)}{d\hat{s}}-\frac{d\Gamma(-S_x)}{d\hat{s}}}{\frac{d\Gamma(S_x)}{d\hat{s}}+\frac{d\Gamma(-S_x)}{d\hat{s}}},\tag{3.3}$$

where the index x is L, T, or N, representing, respectively, the longitudinal asymmetry, the asymmetry in the decay plane, and the normal component to the decay plane. From the definition of the lepton polarization we can see that P_L and P_T are P-odd, T-even, and CP-even observable while P_N is P-even, T-odd, and hence CP-odd observable.[3]

[2]This particular choice of polarization is called helicity.

[3]Because time reversal operation changes the signs of momentum and spin, and parity transformation changes only the sign of momentum.

Our results for the polarization asymmetries are

$$P_L(\hat{s})=\Bigg[\frac{8}{3}m_{B_s}^2\,\mathrm{Re}(A^*C+B^*D)\sqrt{1-\frac{4\hat{m}_\ell^2}{\hat{s}}}\hat{s}(1-\hat{s})^2-\frac{128f_{B_s}^2\hat{m}_\ell^2}{m_{B_s}^2}\left(C_{10}+\frac{m_{B_s}^2}{2m_\ell m_b}C_{Q_2}\right)$$
$$\times\left(\frac{m_{B_s}^2}{2m_\ell m_b}C_{Q_1}\right)\frac{1}{(1-\hat{s})^2(\hat{s}-4\hat{m}_\ell^2)}\Bigg\{(\hat{s}-4\hat{m}_\ell^2\hat{s}-2\hat{s}^2-4\hat{m}_\ell^2\hat{s}^2+3\hat{s}^3)\sqrt{1-\frac{4\hat{m}_\ell^2}{\hat{s}}}$$
$$+(2\hat{m}_\ell^2-8\hat{m}_\ell^4-\hat{s}+8\hat{m}_\ell^2\hat{s}-8\hat{m}_\ell^4\hat{s}+2\hat{m}_\ell^2\hat{s}^2-\hat{s}^3)\ln(\hat{z})\Bigg\}$$
$$+32f_{B_s}\hat{m}_\ell^2\left(C_{10}+\frac{m_{B_s}^2}{2m_\ell m_b}C_{Q_2}\right)\frac{1}{(4\hat{m}_\ell^2-\hat{s})}\Bigg\{\mathrm{Re}(B)\left(-\hat{s}+3\hat{s}^2\right)\sqrt{1-\frac{4\hat{m}_\ell^2}{\hat{s}}}+2(\hat{m}_\ell^2+\hat{m}_\ell^2\hat{s}-\hat{s}^2)\ln(\hat{z})\Bigg)$$
$$-\mathrm{Re}(C)(1-\hat{s})\left(\hat{s}\sqrt{1-\frac{4\hat{m}_\ell^2}{\hat{s}}}+(2\hat{m}_\ell^2-\hat{s})\ln(\hat{z})\right)\Bigg\}+32f_{B_s}\left(\frac{m_{B_s}^2}{2m_\ell m_b}C_{Q_1}\right)\frac{\hat{m}_\ell^2(1-\hat{s})}{\hat{s}\left(1-\frac{4\hat{m}_\ell^2}{\hat{s}}\right)}$$
$$\times\left\{\mathrm{Re}(A)\left(-\hat{s}\sqrt{1-\frac{4\hat{m}_\ell^2}{\hat{s}}}+2\hat{m}_\ell^2\ln(\hat{z})\right)+\mathrm{Re}(D)\left(\hat{s}\sqrt{1-\frac{4\hat{m}_\ell^2}{\hat{s}}}+(2\hat{m}_\ell^2-\hat{s})\ln(\hat{z})\right)\right\}\Bigg]/\Delta, \tag{3.4}$$

$$P_T(\hat{s})=\pi\hat{m}_l\Bigg[-2m_{B_s}^2\,\mathrm{Re}(A^*B)\sqrt{\hat{s}}(1-\hat{s})^2-\frac{64f_{B_s}^2}{m_{B_s}^2}\hat{m}_\ell\left(C_{10}+\frac{m_{B_s}^2}{2m_\ell m_b}C_{Q_2}\right)\left(\frac{m_{B_s}^2}{2m_\ell m_b}C_{Q_1}\right)\frac{(1-4\hat{m}_\ell^2)}{(1-\hat{s})}$$
$$+8f_{B_s}\left(C_{10}+\frac{m_{B_s}^2}{2m_\ell m_b}C_{Q_2}\right)\left\{\mathrm{Re}(B)\,\frac{(1-\hat{s})(\hat{s}+4\hat{m}_\ell^2)}{(2\hat{m}_\ell+\sqrt{\hat{s}})}+\mathrm{Re}(C)(-2\hat{m}_\ell+\sqrt{\hat{s}})(1+\hat{s})\right\}$$
$$+8f_{B_s}\left(\frac{m_{B_s}^2}{2m_\ell m_b}C_{Q_1}\right)\left\{\mathrm{Re}(A)\,\frac{(4\hat{m}_\ell^2+\hat{s}-12\hat{m}_\ell^2\hat{s}+\hat{s}^2)}{(2\hat{m}_\ell+\sqrt{\hat{s}})}-\mathrm{Re}(D)(2\hat{m}_\ell-\sqrt{\hat{s}})(1-\hat{s})\right\}\Bigg]/\Delta, \tag{3.5}$$

$$P_N=\pi\hat{m}_\ell\Bigg[-m_{B_s}^2\,\mathrm{Im}(A^*D+B^*C)(1-\hat{s})^2\sqrt{\hat{s}-4\hat{m}_\ell^2}$$
$$+8f_{B_s}\left(C_{10}+\frac{m_{B_s}^2}{2m_\ell m_b}C_{Q_2}\right)\frac{\hat{s}\sqrt{1-\frac{4\hat{m}_\ell^2}{\hat{s}}}}{(2\hat{m}_\ell+\sqrt{\hat{s}})}\{\mathrm{Im}(A)(1+\hat{s})+\mathrm{Im}(D)(1-\hat{s})\}$$
$$+8f_{B_s}\left(\frac{m_{B_s}^2}{2m_\ell m_b}C_{Q_1}\right)\frac{\sqrt{\hat{s}-4\hat{m}_\ell^2}}{(2\hat{m}_\ell+\sqrt{\hat{s}})}\{\mathrm{Im}(B)(1-\hat{s})+\mathrm{Im}(C)(1-8\hat{m}_\ell^2+\hat{s})\}\Bigg]/\Delta, \tag{3.6}$$

with Δ as defined in Eq. (3.1) and $\hat{m}_\ell=m_\ell/m_{B_s}$.

IV. NUMERICAL RESULTS AND DISCUSSION

We have performed the numerical analysis of various polarization asymmetries whose analytical expressions are given in Eqs. (3.4)–(3.6).

Although MSSM is the simplest (and the one having the least number of parameters) SUSY model, it still has a very large number of parameters making it rather difficult to do any meaningful phenomenology in such a large parameter space. Many choices are available to reduce such a large number of parameters. The most favorite among them is the supergravity (SUGRA) model. In this model, universality of

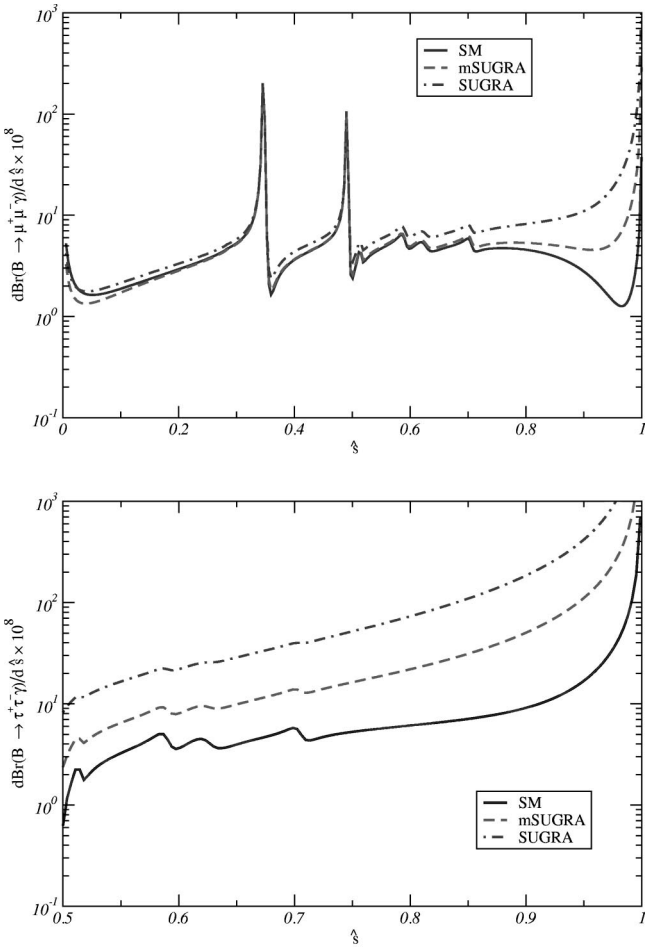

FIG. 1. Branching ratios for $B_s \to \ell^+ \ell^- \gamma$ with $\ell = \mu$ (above) and $\ell = \tau$ (below). MSUGRA parameters are $m = 200$ GeV, $M = 450$ GeV, $A = 0$, and $\tan\beta = 40$. An additional parameter for SUGRA (the pseudo-scalar Higgs mass) is taken to be $m_A = 306$ GeV.

all the masses and couplings is assumed at the grand unified theory (GUT) scale. The minimal SUGRA (MSUGRA) model has only five parameters (in addition to SM parameters) to deal with. They are: m (the unified mass of all the scalars), M (unified mass of all the gauginos), $\tan\beta$ (ratio of vacuum expectation values of the two Higgs doublets), A (the universal trilinear coupling constant), and finally, sgn(μ).[4]

It has been well emphasized in many works [6,9,10] that it is not necessary to have a common mass for all the scalars at the GUT scale. To have required suppression in $K^0 - \overline{K}^0$ mixing, it is sufficient to have common masses of all the squarks at the GUT scale. So the condition of universality of all scalar masses at the GUT is not a very strict one in SUGRA. Thus we also explore a more relaxed kind of MSUGRA model where the condition of universality of all the scalar masses at the GUT scale is relaxed with the assumption that universal squark and Higgs boson masses are different. For the Higgs sector we take the pseudoscalar Higgs boson mass (m_A) to be a parameter. Over the whole MSSM parameter space we have imposed a 95% C.L. bound [23], consistent with CLEO and ALEPH results:

$$2 \times 10^{-4} < \mathrm{Br}(B \to X_s \gamma) < 4.5 \times 10^{-5}.$$

Figure 1 shows plots of the differential braching ratios of $B_s \to \ell^+ \ell^- \gamma$ for leptons to be μ and τ. The prediction of the branching ratios for $B_s \to \ell^+ \ell^- \gamma$ are shown in Table I.

TABLE I. Branching ratios for $B_s \to \ell^+ \ell^- \gamma$ ($\ell = \mu, \tau$).

Model	Br($B_s \to \mu^+ \mu^- \gamma$)	Br($B_s \to \tau^+ \tau^- \gamma$)
Standard model	5.53×10^{-8}	6.57×10^{-8}
MSUGRA[a]	6.86×10^{-8}	3.59×10^{-7}
SUGRA[a]	1.21×10^{-7}	1.31×10^{-6}

[a]The MSUGRA and SUGRA parameters are defined in Fig. 1. These values are of the same order as estimated by Xiong *et al.* [7].

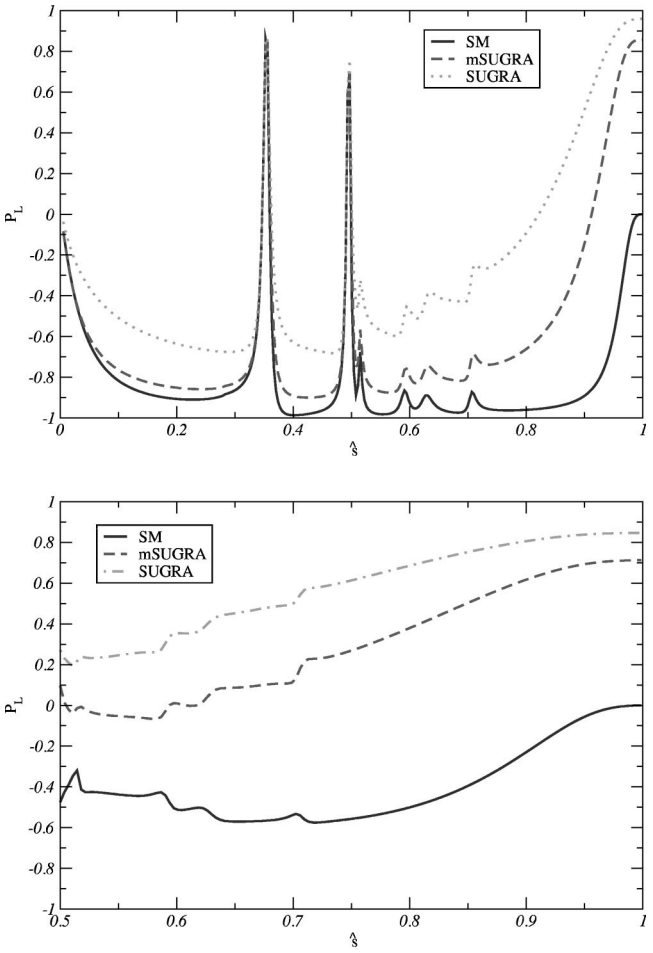

FIG. 2. Longitudinal polarization asymmetry for $B_s \to \ell^+ \ell^- \gamma$ with $\ell = \mu$ (above) and $\ell = \tau$ (below). MSUGRA parameters are $m = 200$ GeV, $M = 450$ GeV, $A = 0$, and $\tan\beta = 40$. An additional parameter for SUGRA (the pseudo-scalar Higgs mass) is taken to be $m_A = 306$ GeV.

[4]Our convention of the sgn(μ) is that μ enters the chargino mass matrix with a positive sign.

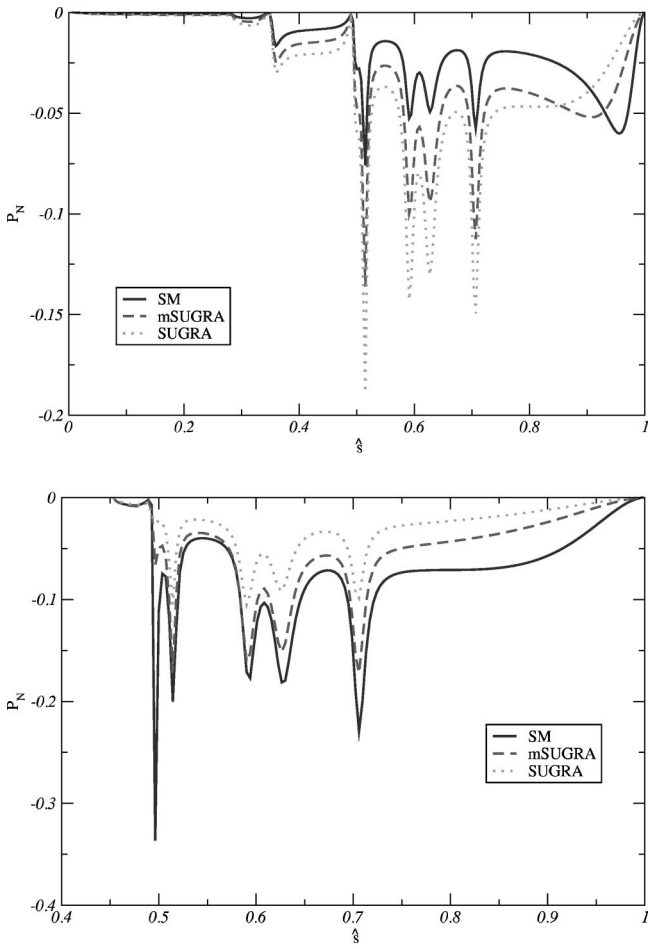

FIG. 3. Normal polarization asymmetry for $B_s \to \ell^+ \ell^- \gamma$ with $\ell = \mu$ (above) and $\ell = \tau$ (below). MSUGRA parameters are $m = 200$ GeV, $M = 450$ GeV, $A = 0$, and $\tan\beta = 40$. An additional parameter for SUGRA (the pseudo-scalar Higgs mass) is taken to be $m_A = 306$ GeV.

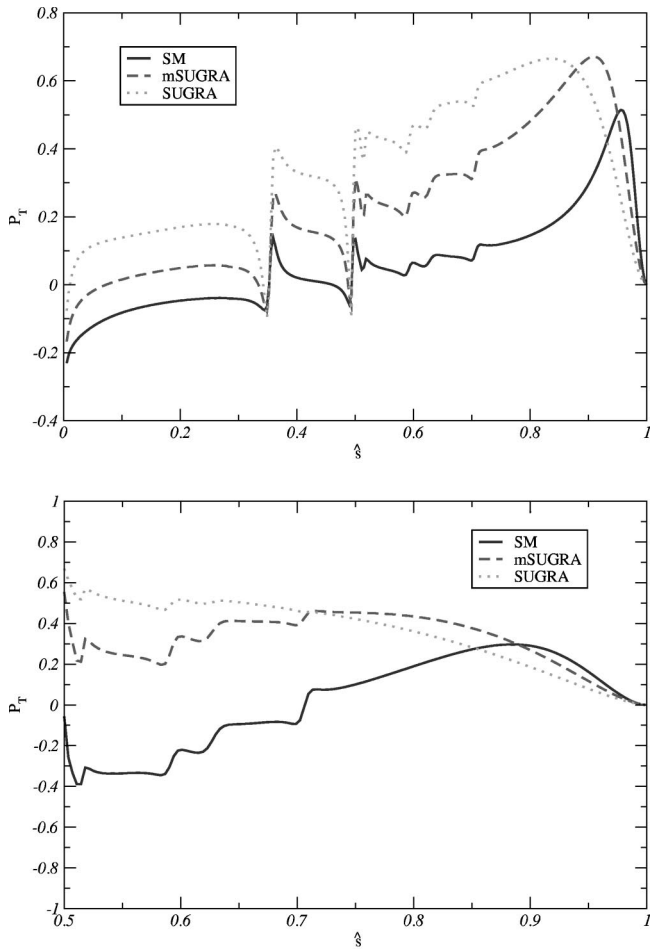

FIG. 4. Transverse polarization asymmetry for $B_s \to \ell^+ \ell^- \gamma$ with $\ell = \mu$ (above) and $\ell = \tau$ (below). MSUGRA parameters are $m = 200$ GeV, $M = 450$ GeV, $A = 0$, and $\tan\beta = 40$. An additional parameter for SUGRA (the pseudo-scalar Higgs mass) is taken to be $m_A = 306$ GeV.

We have plotted various polarization asymmetries (P_L, P_T, and P_N) in the three models: SM, MSUGRA, and SUGRA in Figs. 2–4 for $B_s \to \mu^+ \mu^- \gamma$ and $B_s \to \tau^+ \tau^- \gamma$ as a function of $\hat{s}$ (scaled invariant mass of the dilepton pair).

Now we try to analyze the behavior of the polarization asymmetries on the parameters of the models chosen (MSUGRA and SUGRA). For this analysis we consider the polarization asymmetries at dilepton invariant mass ($\hat{s}$) away from the resonances (the J/Ψ resonances) (we choose $\hat{s} = 0.68$ for our analysis). The main focus of the analysis is NHB effects on polarization asymmetries. These effects crucially depend on $\tan\beta$ and pseudoscalar Higgs boson mass (m_A).

In the MSUGRA model the Higgs boson mass (at electroweak scale) depends crucially on the universal mass of the scalars and $\tan\beta$. To illustrate this crucial behavior, we have plotted various polarization asymmetries as a function of $\tan\beta$ for different values of unified scalar mass (m) in Figs. 5–7. As can be seen from these figures, P_L shows large deviations from the SM values and over a significant portion of the allowed region even shows a sign flip provided $\tan\beta$ is sufficiently large. Similar behavior is also there for P_T. On the other hand, the predictions for P_N do not differ substantially from SM results but the MSUGRA predictions can change P_N by more than 50% with an appreciable increase in $\tan\beta$.

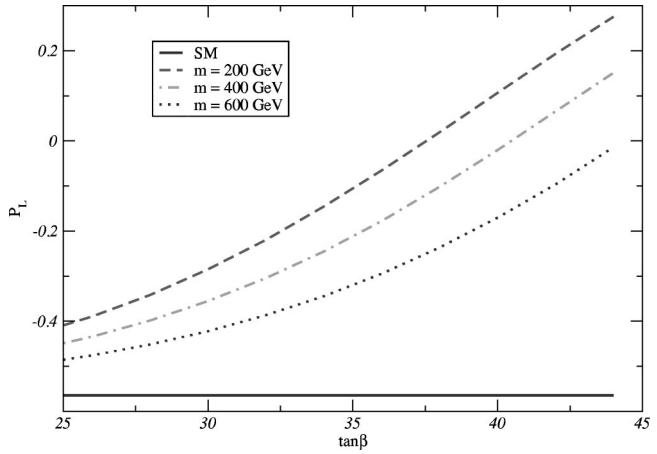

FIG. 5. P_L vs $\tan\beta$ at $\hat{s} = 0.68$ for $B_s \to \tau^+ \tau^- \gamma$ in the MSUGRA model, other parameters are $M = 450$ GeV and $A = 0$.

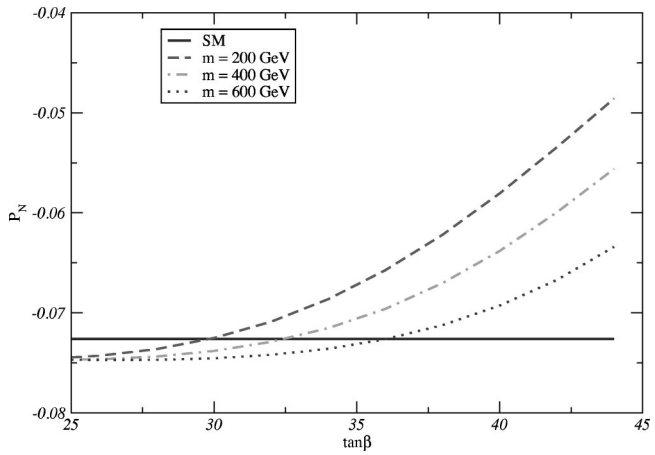

FIG. 6. P_N vs $\tan\beta$ for $B_s \to \tau^+\tau^-\gamma$ at $\hat{s}=0.68$ in MSUGRA, other parameters are $M=450$ GeV and $A=0$.

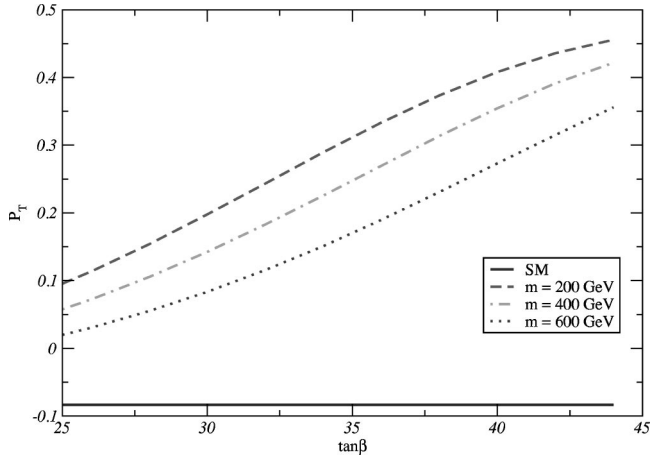

FIG. 7. P_T vs $\tan\beta$ for $B_s \to \tau^+\tau^-\gamma$ at $\hat{s}=0.68$ in MSUGRA, other parameters are $M=450$ GeV and $A=0$.

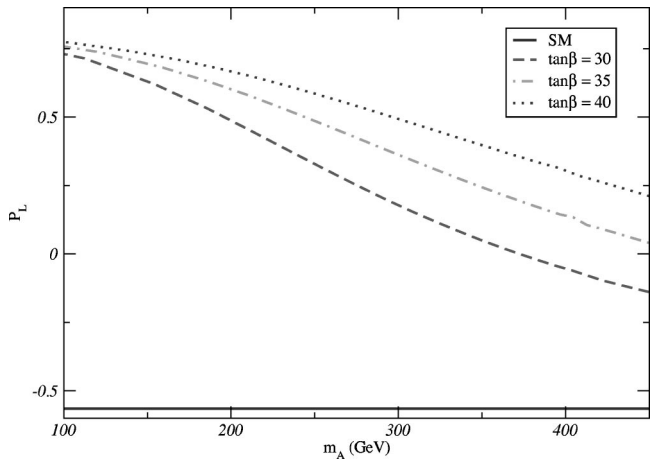

FIG. 8. P_L vs m_A at $\hat{s}=0.68$ for $B_s \to \tau^+\tau^-\gamma$ in SUGRA, other parameters are $m=200$ GeV, $M=450$ GeV, and $A=0$.

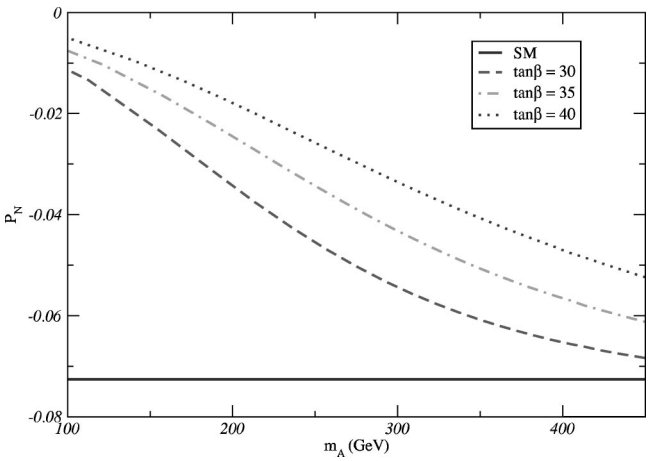

FIG. 9. P_N vs m_A at $\hat{s}=0.68$ for $B_s \to \tau^+\tau^-\gamma$ in SUGRA, other parameters are $m=200$ GeV, $M=450$ GeV, and $A=0$.

For the SUGRA model we have plotted (Figs. 8–10) the polarization asymmetries as a function of pseudoscalar Higgs boson mass (m_A) for various values of $\tan\beta$. In SUGRA we expect more variation of all the polarization asymmetries as compared to their SM values because here we have Higgs boson mass (pseudoscalar Higgs mass) as an additional parameter along with $\tan\beta$. As we can see from Fig. 8 the variation of P_L is more substantial in the SUGRA model. In fact for a fairly large region of SUGRA parameter space, P_L can be opposite in sign as compared to the SM case. P_T can vary up to five in magnitude when compared with the SM value over the large region of allowed parameter space, and for the parameter space we have taken into consideration, the predicted value of P_T in SUGRA is opposite in sign to the SM value. Again P_N does not show as much deviation as observed for P_L and P_T but the variation can still be up to an order in certain regions.

Summarizing the results of the numerical analysis.

(1) From Figs. 2 and 4 it is clear that the longitudinal and transverse polarization asymmetries (P_L,P_T) can have substantial deviation from their respective standard model val-

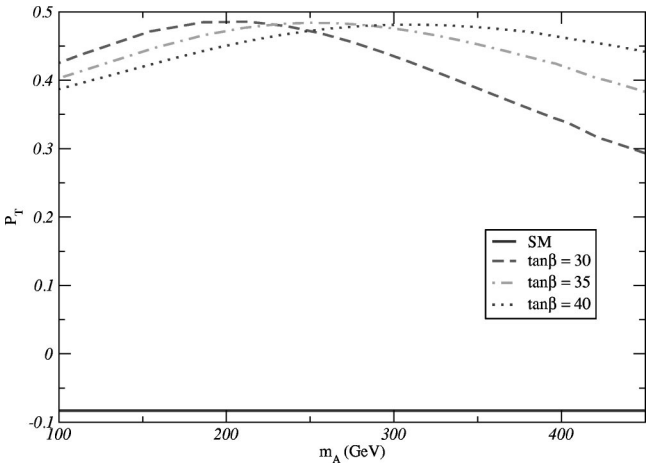

FIG. 10. P_T vs m_A for $B_s \to \tau^+\tau^-\gamma$ at $\hat{s}=0.68$ in SUGRA, other parameters are $m=200$ GeV, $M=450$ GeV, and $A=0$.

ues over the whole region of dilepton invariant mass ($\hat{s}$), while Fig. 3 indicates deviation for P_N from SM values for a limited region of the dilepton invariant mass.

(2) As we have pointed out earlier [9], for the inclusive process $B\to X_s\ell^+\ell^-$ there is not much deviation from SM results in the MSUGRA model. But in the radiative dileptonic decay mode, MSUGRA predictions also show large deviations (at least of P_L and P_T) from SM results, making it possible to use polarization asymmetries to test the MSUGRA model. This is mainly because in the bremmstrahlung part of the matrix element ($\mathcal{M}_2$), the Wilson coefficient C_{Q_2} adds on to C_{10} via the combination $(C_{10}+m_{B_s}^2/2m_\ell m_b C_{Q_2})$ which effectively increases the SM value of C_{10}. This does not happen for the process $B\to X_s\ell^+\ell^-$ and this numerically is the reason for the scalar exchanges affecting the $B_s\to\ell^+\ell^-\gamma$ process more than the semileptonic one.

(3) From Figs. 5–7 we can see that the polarization asymmetries show a general enhancement with an increase in $\tan\beta$ and they decrease as the universal scalar mass (m) is increased. This is expected because the Higgs boson mass increases with m and thus the contributions of scalar (C_{Q_1}) and pseudoscalar (C_{Q_2}) type interactions decrease.

(4) As can be seen from the structure of the analytical expressions for various polarization asymmetries [Eqs. (3.4), (3.5), and (3.6)], they are all different analytic functions of various Wilson coefficients and hence contain independent information. These asymmetries, hence, can also be used for accurate determination of various Wilson coefficients.

In conclusion, we can say that the observation of the polarization asymmetries can be a very useful probe for finding out the new physics effects and testing the structure of the effective Hamiltonian.

ACKNOWLEDGMENT

N.M. would like to thank the University Grants Commission, India for financial support.

APPENDIX A: INPUT PARAMETERS

$$m_{B_s}=5.26\ \text{GeV},\quad m_c=1.4\ \text{GeV},\quad m_s=0.2\ \text{GeV},$$

$$m_\mu=0.106\ \text{GeV},\quad m_\tau=1.77\ \text{GeV},\quad m_b=4.8\ \text{GeV},$$

$$m_w=80.4\ \text{GeV},\quad m_t=176\ \text{GeV},\quad |V_{tb}V_{ts}^*|=0.045,$$

$$G_F=1.17\times10^{-5}\ \text{GeV}^{-2},\quad \alpha=\frac{1}{129},$$

$$\tau(m_{B_s})=1.6\times10^{-12}\ \text{s}.$$

APPENDIX B

The definitions of A, B, C, and D defined in Eq. (2.3) are

$$A=\frac{1}{m_{BS_s}^2}\left[C_9^{\text{eff}}G_1(p^2)-2C_7^{\text{eff}}\frac{m_b}{p^2}G_2(p^2)\right],$$

$$B=\frac{1}{m_{B_s}^2}\left[C_9^{\text{eff}}F_1(p^2)-2C_7^{\text{eff}}\frac{m_b}{p^2}F_2(p^2)\right],$$

$$C=\frac{C_{10}}{m_{B_s}^2}G_1(p^2),$$

$$D=\frac{C_{10}}{m_{B_s}^2}F_1(p^2), \tag{B1}$$

where the form factors definition chosen is [22]

$$\langle\gamma|\bar{s}\gamma_\mu(1\pm\gamma_5)b|B_s\rangle=\frac{e}{m_{B_s}^2}\{\varepsilon_{\mu\alpha\beta\sigma}\epsilon_\alpha^* p_\beta q_\sigma G_1(p^2) \mp i[(\epsilon_\mu^*(pq)-(\epsilon^* p)q_\mu)]F_1(p^2)\}, \tag{B2}$$

$$\langle\gamma|\bar{s}i\sigma_{\mu\nu}p_\nu(1\pm\gamma_5)b|B_s\rangle = \frac{e}{m_{B_s}^2}\{\varepsilon_{\mu\alpha\beta\sigma}\epsilon_\alpha^* p_\beta q_\sigma G_2(p^2) \pm i[(\epsilon_\mu^*(pq)-(\epsilon^* p)q_\mu)] \times F_2(p^2)\}. \tag{B3}$$

Multiplying Eq. (B2) with p_μ and using equation of motion we can get the relation

$$\langle\gamma|\bar{s}(1\pm\gamma_5)b|B_s\rangle=0. \tag{B4}$$

The definition of form factors we are using for numerical analysis is [22]

$$G_1(p^2)=\frac{1}{1-p^2/5.6^2}\text{GeV},\quad G_2(p^2)=\frac{3.74}{1-p^2/40.5}\text{GeV}^2,$$
$$F_1(p^2)=\frac{0.8}{1-p^2/6.5^2}\text{GeV},\quad F_2(p^2)=\frac{0.68}{1-p^2/30}\text{GeV}^2. \tag{B5}$$

Identities used in the calculation of the matrix element when a photon is radiated from the lepton leg:

$$\langle0|\bar{s}b|B_s\rangle=0, \tag{B6}$$

$$\langle0|\bar{s}\sigma_{\mu\nu}(1+\gamma_5)b|B_s\rangle=0, \tag{B7}$$

$$\langle0|\bar{s}\gamma_\mu\gamma_5 b|B_s\rangle=-if_{B_s}P_{B_s\mu}. \tag{B8}$$

[1] A. Ali, hep-ph/9709507; G. Buchalla, A. J. Buras, and M. E. Lautenbacher, Rev. Mod. Phys. **68**, 1125 (1996).
[2] E. O. Iltan and G. Turan, Phys. Rev. D **61**, 034010 (2000); G. Erkol and G. Turan, Acta Phys. Pol. B **33**, 1285 (2002).
[3] T. M. Aliev and M. Savci, Phys. Lett. B **452**, 318 (1999).
[4] W. Skiba and J. Kalinowski, Nucl. Phys. **B404**, 3 (1993); H. E. Logan and U. Nierste, *ibid.* **B586**, 39 (2000).
[5] Y. Dai, C. Huang, and H. Huang, Phys. Lett. B **390**, 257 (1997).
[6] S. R. Choudhury and N. Gaur, Phys. Lett. B **451**, 86 (1999); D. A. Demir, K. A. Olive, and M. B. Voloshin, Phys. Rev. D **66**, 034015 (2002); C. Bobeth, T. Ewerth, F. Krüger, and J. Urban, *ibid.* **64**, 074014 (2001).
[7] Z. Xiong and J. M. Yang, Nucl. Phys. **B628**, 193 (2002).
[8] C. Huang, W. Liao, and Q. Yan, Phys. Rev. D **59**, 011701 (1999).
[9] S. Rai Choudhury, A. Gupta, and N. Gaur, Phys. Rev. D **60**, 115004 (1999).
[10] T. Goto, Y. Okada, Y. Shimizu, and M. Tanaka, Phys. Rev. D **55**, 4273 (1997); T. Goto, Y. Okada, and Y. Shimizu, *ibid.* **58**, 094006 (1998).
[11] C. Bobeth, A. J. Buras, F. Kruger, and J. Urban, Nucl. Phys. **B630**, 87 (2002).
[12] P. L. Cho, M. Misiak, and D. Wyler, Phys. Rev. D **54**, 3329 (1996).
[13] J. L. Hewett and J. D. Wells, Phys. Rev. D **55**, 5549 (1997).
[14] CLEO Collaboration, M. S. Alam *et al.*, Phys. Rev. Lett. **74**, 2885 (1995); CLEO Collaboration, R. Ammar *et al.*, *ibid.* **71**, 674 (1993).
[15] Y. Grossman, Z. Ligeti, and E. Nardi, Phys. Rev. D **55**, 2768 (1997).
[16] G. Eilam, C. Lu, and D. Zhang, Phys. Lett. B **391**, 461 (1997).
[17] T. M. Aliev, A. Özpineci, and M. Savci, Phys. Rev. D **55**, 7059 (1997); T. M. Aliev, N. K. Pak, and M. Savci, Phys. Lett. B **424**, 175 (1998).
[18] Y. Dincer and L. M. Sehgal, Phys. Lett. B **521**, 7 (2001); C. Q. Geng, C. C. Lih, and W. M. Zhang, Phys. Rev. D **62**, 074017 (2000).
[19] F. Krüger and L. M. Sehgal, Phys. Lett. B **380**, 199 (1996); J. L. Hewett, Phys. Rev. D **53**, 4964 (1996).
[20] B. Grinstein, M. J. Savage, and M. B. Wise, Nucl. Phys. **B319**, 271 (1989); A. J. Buras and M. Münz, Phys. Rev. D **52**, 186 (1995).
[21] A. Ali, T. Mannel, and T. Morozumi, Phys. Lett. B **273**, 505 (1991); C. S. Lim, T. Morozumi, and A. I. Sanda, *ibid.* **218**, 343 (1989); N. G. Deshpande, J. Trampetic, and K. Panose, Phys. Rev. D **39**, 1461 (1989); P. J. O'Donnell and H. K. Tung, *ibid.* **43**, 2067 (1991).
[22] G. Eilam, I. Halperin, and R. R. Mendel, Phys. Lett. B **361**, 137 (1995); G. Buchalla and A. J. Buras, Nucl. Phys. **B400**, 225 (1993).
[23] K. Anikeev *et al.*, ''B Physics at Tevatron: Run II & Beyond,'' hep-ph/0203041; CLEO Collaboration, T. E. Coan *et al.*, Phys. Rev. Lett. **84**, 5283 (2000); ALEPH Collaboration, R. Barate *et al.*, Phys. Lett. B **429**, 169 (1998).